

7th International Conference on Silicon Photovoltaics, SiliconPV 2017

# Minority carrier lifetimes in Cz-Si wafers with intentional V-I transitions

Rune Søndena<sup>a\*</sup>, Birgit Ryningen<sup>b</sup>, Mari Juel<sup>b</sup>

<sup>a</sup>*Institute for Energy Technology, Instituttveien 18, N-2007, Kjeller, Norway*

<sup>b</sup>*SINTEF Materials and Chemistry, Richard Birkelandsvei 2b, N-7491, Trondheim, Norway*

---

## Abstract

A p-type Cz-Si crystal has been pulled with varying pulling speed in order to produce wafers containing two distinct regions; A region with silicon self-interstitial defects, and a vacancy dominated region. Band-to-band photoluminescence imaging has been used to study the minority charge carrier lifetimes in these wafers after different processing steps. Despite the different defects found in the different regions of the wafers carrier lifetimes appear to be uniform across the entire wafers, both for ungettered and gettered samples. Only after an oxidation process at 1100 °C oxygen related ring patterns become visible. It is, however, difficult to identify the band structure of the transition area between the regions among all the striations in the crystal.

© 2017 The Authors. Published by Elsevier Ltd.

Peer review by the scientific conference committee of SiliconPV 2017 under responsibility of PSE AG.

**Keywords:** Czochralski; Defects; Impurities; Degradation

---

## 1. Introduction

Microdefects such as silicon self-interstitials (I) and vacancies (V) are incorporated into the Czochralski (Cz) silicon during crystallization.[1-4] Void formation and impurity agglomeration, both during the crystal growth and the later high temperature processing are important for determining the electrical properties of the silicon material. According to the *Voronkov criterion* the dominant microdefect type is largely determined by the  $v/G$  ratio, where  $v$  is the pulling speed and  $G$  is a temperature gradient near the solid-liquid interface during crystal pulling. Due to the equilibrium conditions, defect recombination and the respective mobilities of I and V, silicon self-interstitials

---

\* Corresponding author. Tel.: +47 920 29 610.

E-mail address: [rune.sondena@ife.no](mailto:rune.sondena@ife.no)

dominate below and vacancies above a critical value of about  $(v / G)_{critical} = 0.134 \text{ mm}^2 \text{ min}^{-1} \text{ K}^{-1}$ . [5-7] At the interface between the V and I dominated regions a transition area forms. This so-called p-band can be traced by several methods, e.g. by Cu-decoration or by inducing stacking faults by oxidation. [8-11] In addition to the microdefects oxygen originating from the quartz crucible containing the melt is incorporated into the crystal during the solidification. Cz-Si can contain as much as  $10^{18} \text{ cm}^{-3}$  interstitial oxygen that again may form more detrimental defect complexes and agglomerates. [12-17]

Crystalline silicon wafers containing both boron and oxygen generally exhibit a considerable degradation of the minority charge carrier lifetime (hereafter referred to as lifetime) upon prolonged carrier injection, e.g. under illumination. Within a day or two of illumination the lifetimes are typically reduced to about 10% of the initial lifetime. [18] This light induced degradation (LID) has been attributed the  $\text{BO}_2$ -complex. However, neither the exact chemical composition nor the energy level of the defect in the band gap has been determined experimentally. A normalized defect concentration,  $N_t^*$ , is therefore used in order to quantify the BO-related LID.

$$N_t^* = \frac{1}{\tau_{degraded}} - \frac{1}{\tau_{initial}} \quad (1)$$

where  $\tau_{initial/degraded}$  are the lifetimes before and after light induced degradation, respectively. [19,20] According to Shockley-Read-Hall (SRH) theory, Eq. 1 is valid only if the BO-complex is the main lifetime limiting defect. [21,22]

In the present work wafers containing both V- and I-dominated regions are studied with respect to their minority carrier lifetimes. Band-to-band photoluminescence imaging is used to evaluate the spatial differences in the lifetimes and the decay thereof.

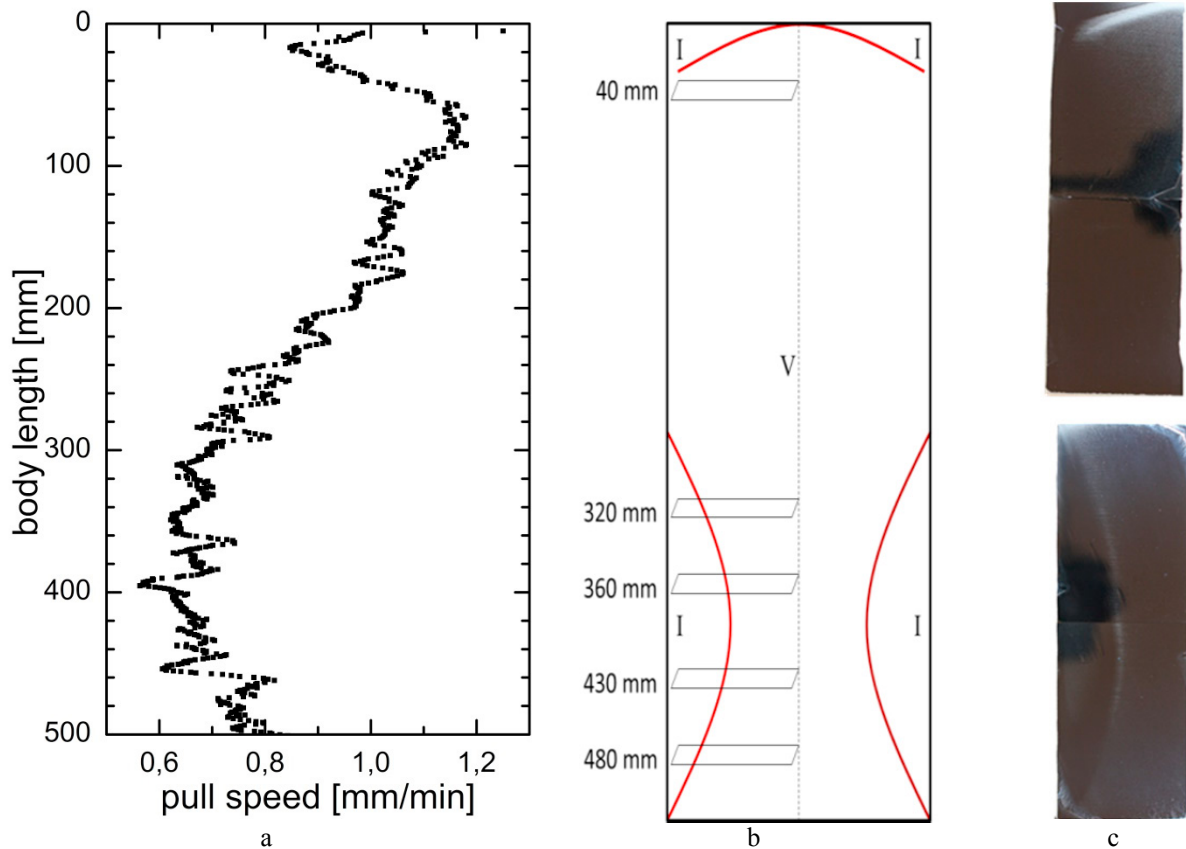


Fig. 1. The varying pull speed through the length of the crystal is shown in a). Vacancy and interstitial rich areas and the p-band marking the transition are indicated in b) together with the approximate wafer positions. The actual p-band found using Cu-decoration is shown in c).

## 2. Experimental details

A boron doped 6 inch p-type Cz crystal was grown in the  $\langle 100 \rangle$  direction. The pulling speed was varied according to Figure 1a in order to generate a V-I transition not only in the shoulder region of the crystal near the seed end but also running down the main body of the crystal. Half the crystal is wafered into  $5 \times 5 \text{ cm}^2$  wafers while the other half is cut into vertical cross sections. The approximate positions of the wafers studied in the present work are shown in Figure 1b. Copper decoration, i.e. in diffusion of  $\text{Cu}(\text{NO}_3)_2$  at  $900^\circ\text{C}$  followed by Secco-etching, has been performed on vertical samples (Figure 1c).

Wafers from different positions are etched and subjected to different high temperature processes as shown in Figure 2. Ungettered wafers are only damage etched prior to surface passivation. In the gettering process a phosphorus emitter is in-diffused, followed by an emitter etch-back. Wet oxidation is performed at  $1100^\circ\text{C}$  in steam ambient using a Tempress tube furnace.[9,10,23,24] Surface recombination velocities of  $5 \text{ cm/s}$  or less are obtained using PECVD deposited hydrogenated amorphous silicon. QssPC-calibrated photoluminescence imaging was performed using a LIS-R1 setup from BTImaging.[25] BO-related light induced degradation was determined at an injection level,  $\Delta n$ , corresponding to  $0.1 \times p_0$ . The normalized defect concentration,  $N_t^*$ , is then used to quantify the magnitude of the BO-related LID.

Radial and axial interstitial oxygen ( $\text{O}_i$ ) concentrations are measured using FTIR. 2 mm thick vertical cross sections, as seen in Figure 1c, were used.

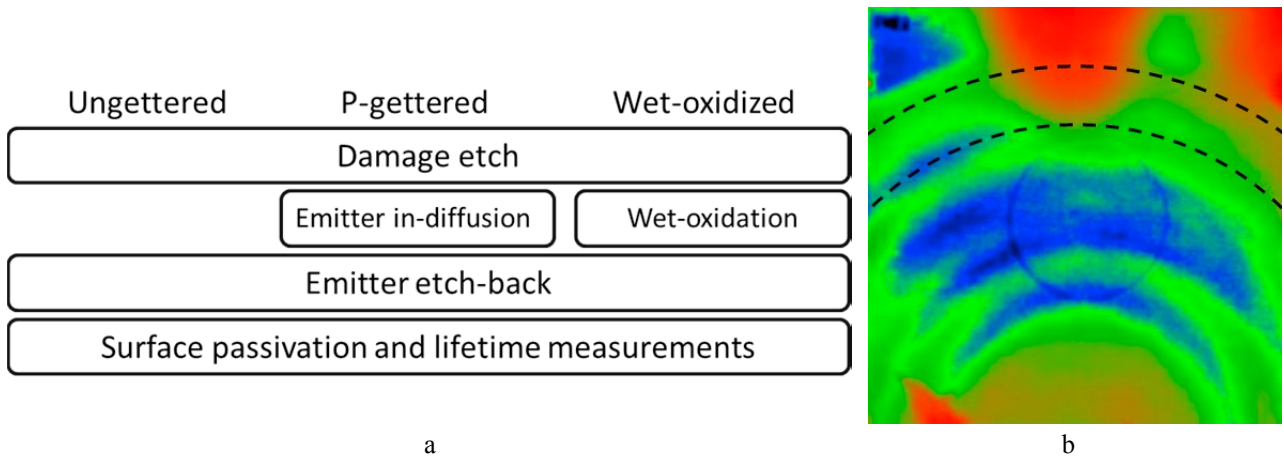


Fig. 2. The different wafer processing routes are shown in a). All wafers are etched together in order to get comparable surface textures prior to the passivation process. The complex ring structure (430 nm) appearing after an oxidation step is shown in b). The p-band is expected to lie within the dashed lines.

## 3. Results

### 3.1. Lifetime measurements

The position of the p-band marking the transition from V to I regions is shown on a vertical sample using copper decoration in Figure 1b. Wafers from 40 mm from the seed end do not contain such a transition, while wafers in the lower half of the crystal all include such ring structures. A wet-oxidized wafer from about 430 mm is shown in Figure 2b. A complex pattern of rings appear after oxidation, and identifying the p-band is somewhat difficult. The approximate position of the p-band based on the position of the wafer and the Cu-decoration in Figure 1c is therefore indicated.

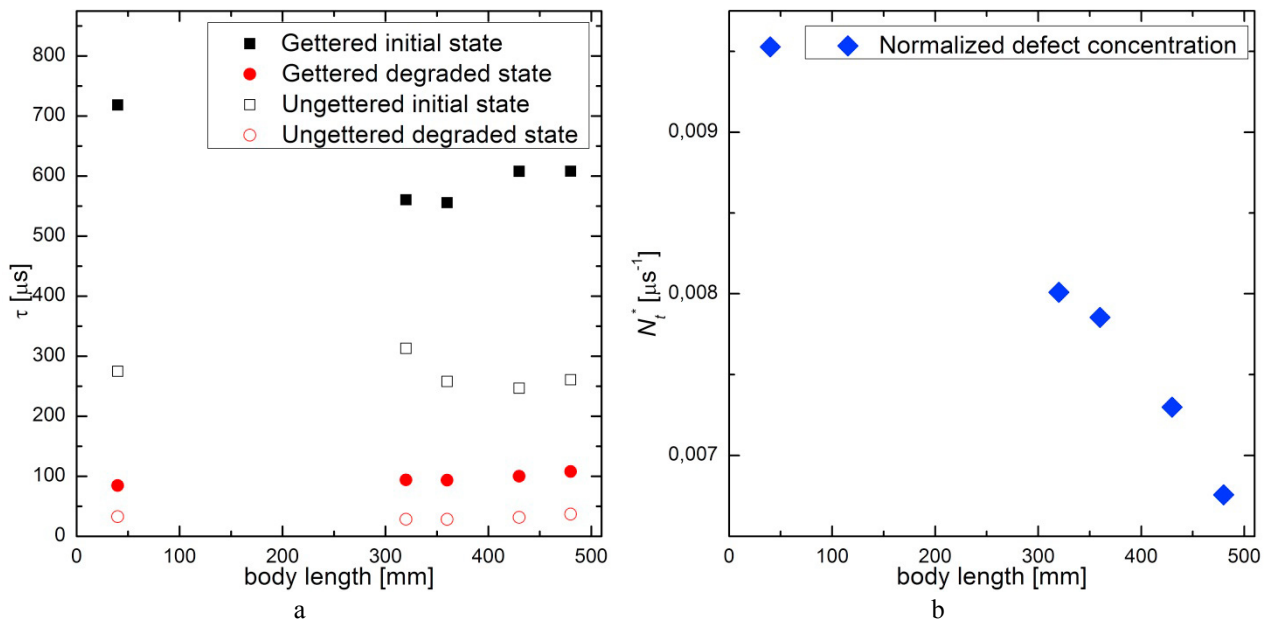


Fig. 3. Initial and degraded minority carrier lifetimes of both ungettered (red) and gettered (black) wafers are shown in a). Initial lifetimes are measured after an annealing at 200 °C and the degraded lifetimes are measured after illumination for 72 hours. The corresponding normalized defect concentrations according to Eq.1, based on the gettered average lifetime values, are shown in b).

Average lifetimes from QssPC calibrated PL-imaging, both initial and after illumination for 72 hours, are shown in Figure 3a. After a phosphorus gettering the measured lifetime is increased considerably for all wafers. Roughly a doubling of the lifetime upon gettering indicates the presence of fast diffusing metallic impurities, e.g. iron, that are removed during the phosphorus in-diffusion. In the initial state the highest lifetimes are measured in the wafer from the seed end, for both ungettered and gettered wafers. Increasing the distance to the seed decreases the lifetime. In the degraded state this difference is not present. For gettered wafers in the degraded state the lifetimes are lowest near the seed, with a clear increase with distance from the seed. This effect is attributed BO-related LID, as the lifetime degrades considerably when exposed to carrier injection (illumination). The largest decay is seen in the wafer closest to the seed, with a degraded lifetime of about 10% of the initial value. A decay of this magnitude is not uncommon in p-type Cz-Si.[18]

Due to different segregation coefficients different impurities distribute differently within a crystal. Boron and metallic impurities will increase with the body length, while oxygen levels normally decrease. The two different trends; decreasing lifetimes with body length end in the initial state, both for gettered and ungettered wafers, and increasing lifetime with the body length in the fully degraded wafers, mainly in gettered wafers, may be explained by different sets of lifetime limiting defects. In the initial state metallic impurities may be the most recombination active defect. As the impurity levels of metallic impurities increase with distance from the seed the lifetimes decrease. As much of the metallic elements are removed in the gettering process, the trend may be less clear on gettered wafers. After illumination BO-complexes are activated, and becomes the main lifetime limiting defect. The degraded lifetimes in the gettered state may represent the decreased oxygen levels towards the tail end in a Cz-Si crystal. Both these recombination paths may contribute to the degraded lifetime in the ungettered degraded state.

Quantification of the light induced degradation using the normalized defect concentration confirms the impression that the LID is decreasing when moving towards the tail of the crystal. Radial linescans showing the  $N_t^*$  in a selection of wafers are presented in Figure 4a. The  $O_i$  concentrations measured at comparable heights using FTIR are shown in Figure 4b. From Figure 3b we know that the  $N_t^*$  decreases with increasing distance from the seed end. This corresponds well with the decreasing levels of  $O_i$  measured towards the tail. The radial linescans also show a general trend of decreasing LID towards the outer edge, with a maximum in the centre of the Cz-crystal. FTIR measurements also confirm that higher levels of interstitial oxygen are measured in the centre of the crystal with decreasing levels towards the outer edges. Elevated  $N_t^*$  values are also seen towards the outer edge (radius > 45

mm), however, this is most likely surface recombination affecting the lifetime, thus, erroneously interpreted as BO-related defects in Equation 1.

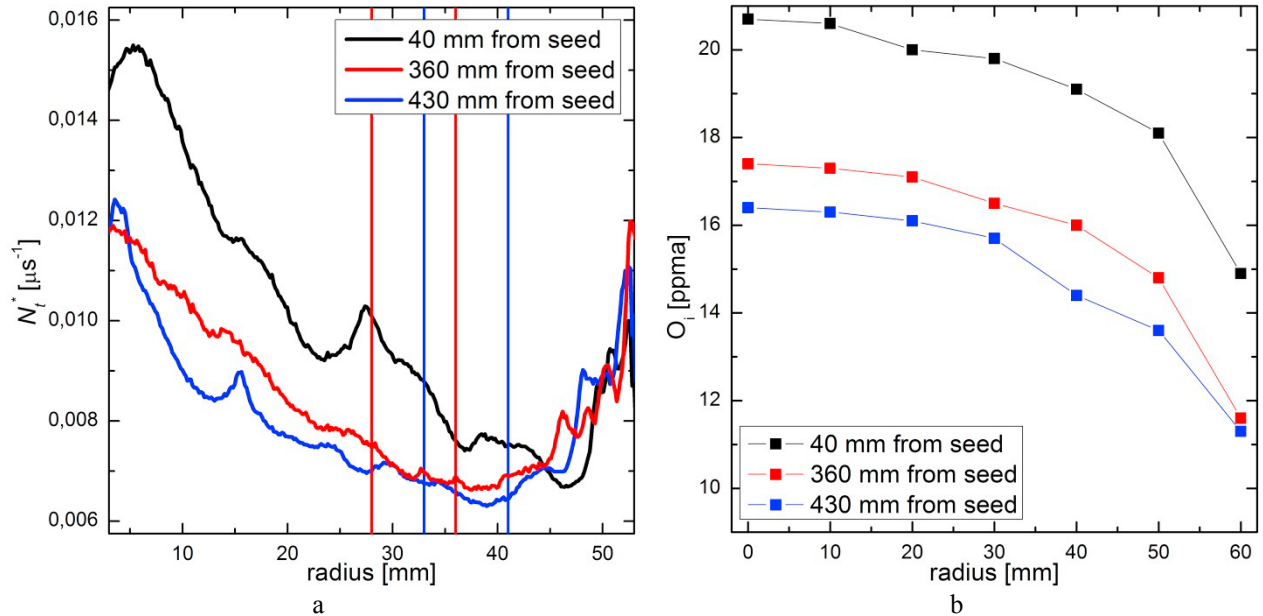


Fig. 4. Normalized defect concentrations used to quantify the BO-related LID. The average value across the whole wafer and a radial linescan are shown in a) and b), respectively. In b) the assumed position of the p-bands are indicated for the different wafer heights.

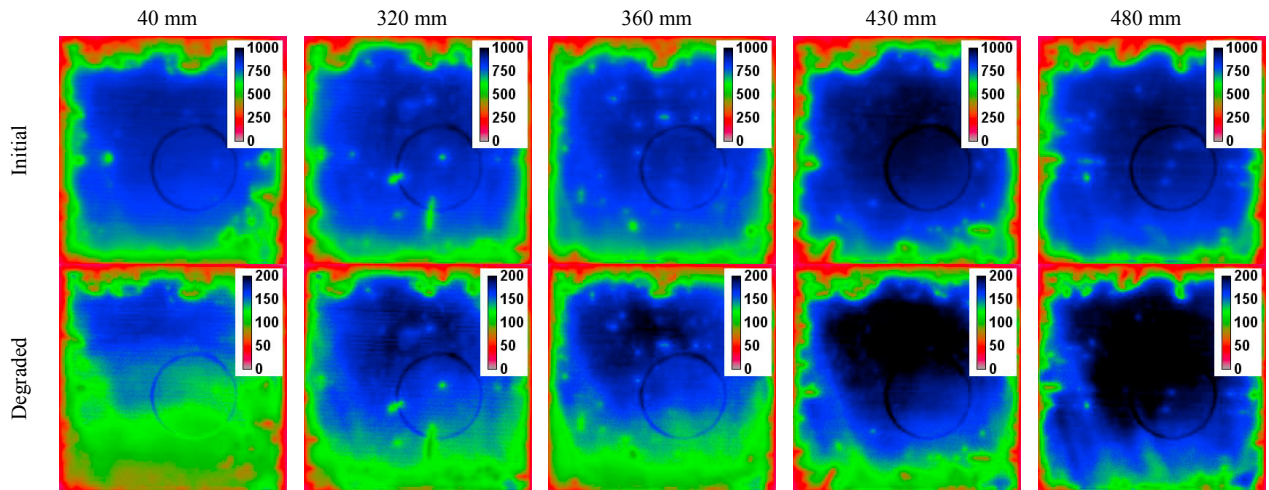


Fig. 5. PL images of the lifetime at an injection level corresponding to  $0.1 \times p_0$ . Initial lifetimes (top) and degraded lifetimes (bottom) for the different positions are shown. The centre of the Cz crystal is located approximately at the middle of the lower edge of the wafers.

Figure 5 shows the spatial distribution of the lifetimes in gettered wafers in the initial state as well as the degraded state. The radial gradient is clearly visible in the degraded state. Wafers from the lower half of the crystal all contain a p-band marking the transition from a V-dominated hemisphere at the lower edge of the wafers to an I-dominated region towards the top of the wafers (see Figure 2b). This p-band is not visible in either the gettered or the ungettered wafers. Since there is no sign of the p-band even in the initial state we can assume that the phosphorus in-diffusion at 833 °C does not result in growth of oxygen precipitates in such an amount as to affect the lifetime. The approximate position of the p-bands are indicated in Figure 4a, showing a radial variation but no



visible transition with respect to the  $N_t^*$  value at the position of the p-bands. Two possible reasons may explain this; Vacancies and interstitials do not affect the oxygen distribution in a sufficient way to affect the BO-degradation, or the effect of vacancies and interstitials is minimal compared to the strong recombination level introduced when the BO-defect is activated. This corresponds well with previous experiments performed by D. Walter et al.[26], Macdonald et al. [27] and Rein et al.[28]

### 3.2. Shockley-Read-Hall modelling

Shockley-Read-Hall (SRH) modelling was performed by fitting defect levels and defect concentrations towards the measured QssPC-curves showing the lifetime as a function of the injection level. Figure 6 represents possible defect configurations, but it does not exclude the possibilities of other, more complex solutions for the same lifetime curve.

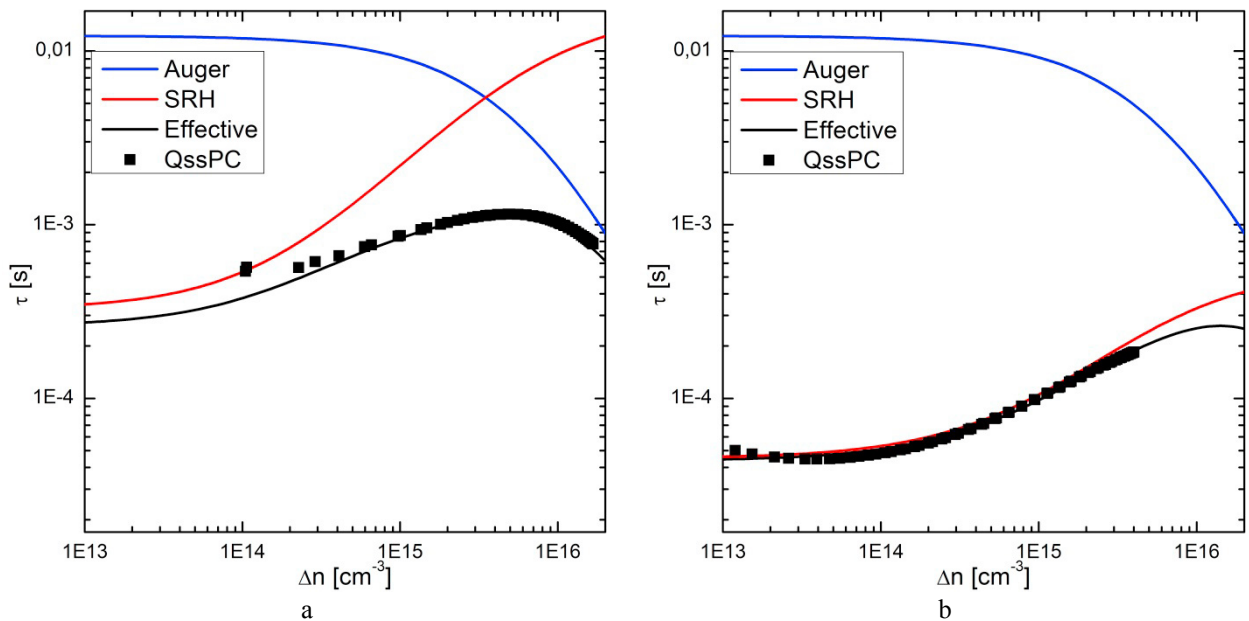


Fig. 6. Injection dependent minority carrier lifetime curves (QssPC) and SRH-modelled lifetime curves for the gettered wafer at 40 mm in a) the initial state and b) the degraded state.

Figure 6a shows the lifetime in a gettered wafer at 40 mm in the initial state. The effective lifetime according to the SRH-theory is obtained with only one impurity added; interstitial iron ( $Fe_i$ ). Literature values for the defect levels and capture cross sections of  $Fe_i$  are taken from the work of Rein and Glunz,[29] also obtained using lifetime spectroscopy. A maximum  $Fe_i$ -concentration of  $8.5 \times 10^{10} \text{ cm}^{-3}$  is found in this gettered wafer. This iron concentration is transferred to the degraded wafer, shown in Figure 6b, where an additional defect is required to reduce modelled lifetime in correspondence with the measured values. We find that one deep defect level between 0.3-0.8 eV above the valence band with an electron/hole capture cross section ratio  $k = \sigma_n/\sigma_p = 9.8$  gives the best fit to the measured data. A similar defect has previously been attributed the BO-defect.[30] However, two defect levels have recently been proposed to describe this very same defect.[31]

## 4. Summary

Cu decoration has been used to demonstrate the presence of a p-band separating a vacancy dominated region and a silicon self-interstitial rich region in a Cz crystal. Wafers containing both V and I dominated regions have been studied with respect to minority carrier lifetimes. Phosphorus gettering has been shown to improve the lifetime considerably revealing the presence of fast diffusing metallic elements in the ungettered wafers. As this is p-type

silicon containing both boron and oxygen, the BO-related LID is the dominating lifetime limiting defect after prolonged illumination, although metallic impurities contribute to reducing the lifetime in ungettered wafers. There is no sign of the p-band in ungettered or gettered wafers. Apparently the emitter in-diffusion does not generate sufficient growth of oxygen agglomerates to affect the lifetime in the p-band. The degraded lifetime in the wafers as well as the LID seems to depend mostly on the oxygen concentrations. Increasing lifetimes are observed with decreasing oxygen levels towards the tail of the crystal and towards the outer edges of each wafer. No visible boundary is observed across the transition from V to I dominated regions.

## Acknowledgements

The present work was performed within *The Norwegian Research Centre for Solar Cell Technology*, co-sponsored by the Norwegian Research Council and research and industry partners in Norway. The authors wish to thank the following people: John Atle Bones and Pål Tetlie (SINTEF) for pulling the Cz-Si ingot and Birgitte Karlsen (SINTEF) for sample preparation and defect etching of vertical cross sections.

## References

- [1] Voronkov VV, Falster R. Grown-in microdefects, residual vacancies and oxygen precipitation bands in Czochralski silicon. *J Cryst Growth* 1999;204:462-474.
- [2] Voronkov VV. The mechanism of swirl defects formation in silicon. *J Cryst Growth* 1982;59:625-643.
- [3] Falster R, Voronkov VV, Quast F. On the properties of the intrinsic point defects in silicon: A perspective from crystal growth and wafer processing. *Phys Status Solidi B-Basic Res* 2000;222:219-244.
- [4] Voronkov VV, Falster R. Vacancy-type microdefect formation in Czochralski silicon. *J Cryst Growth* 1998;194:76-88.
- [5] Voronkov VV. Grown-in defects in silicon produced by agglomeration of vacancies and self-interstitial. *J Cryst Growth* 2008;310:1307-1314.
- [6] Sinno T, Dornberger E, von Ammon W, Brown RA, Dupret F. Defect engineering of Czochralski single-crystal silicon. *Mater Sci Eng R-Reports* 2000;28:149-198.
- [7] von Ammon W, Dornberger E, Oelkrug H, Weidner H. The dependence of bulk defects on the axial temperature gradient of silicon crystals during Czochralski growth. *J Cryst Growth* 1995;151:273-277.
- [8] Mule'Stagno L. A technique for delineating defects in silicon. *Solid State Phenom* 2002;82-84:753-758.
- [9] Søndenå R, Hu Y, Juel M, Wiig MS, Angelskå H. Characterization of the OSF-band structure in n-type Cz-Si using photoluminescence-imaging and visual inspection. *J Cryst Growth* 2013; 367:68-72.
- [10] Angelskå H, Marstein ES, Wiig MS, Søndenå R. Characterization of oxidation induced stacking fault rings in Cz silicon: Photoluminescence imaging and visual inspection after Wright etch. *Energy Procedia* 2012;27:160-166.
- [11] Hu Y, Juel M, E. Øvrelid EJ, Arnberg L. Comparison of different techniques for characterization of defects in n-type Cz silicon. in 26<sup>th</sup> EUPVSEC 2011 Hamburg, Germany.
- [12] Bothe K, Sinton R, Schmidt J. Fundamental boron-oxygen-related carrier lifetime limit in mono- and multicrystalline silicon. *Prog Photovolt* 2005;13:287-296.
- [13] Haunschild J, Reis IE, Geilker J, Rein S. Detecting efficiency-limiting defects in Czochralski-grown silicon wafers in solar cell production using photoluminescence imaging. *Phys Status Solidi-Rapid Res Lett* 2011;5:199-201.
- [14] Murphy JD, Bothe K, Olmo M, Voronkov VV, Falster RJ. The effect of oxide precipitates on minority carrier lifetime in p-type silicon. *J Appl Phys* 2011;110:53713-9.
- [15] Murphy JD, Bothe K, Krain R, Voronkov VV, Falster RJ. Parameterisation of injection-dependent lifetime measurements in semiconductors in terms of Shockley-Read-Hall statistics: An application to oxide precipitates in silicon. *J Appl Phys* 2012;111:113709-10.
- [16] Søndenå R, Holt A, Søiland AK. Electrical properties of compensated n- and p-type monocrystalline silicon. in 26<sup>th</sup> EUPVSEC 2011 Hamburg, Germany.
- [17] Niewelt T, Schön J, Warta W, Glunz SW, Schubert MC. Degradation of crystalline silicon due to boron oxygen defects. *IEEE J Photovolt* 2017;7:383-398.
- [18] Nærlund TU, Haug H, Angelskå H, Søndenå R, Marstein ES, Arnberg L. Studying Light-Induced Degradation by Lifetime Decay Analysis: Excellent Fit to Solution of Simple Second-Order Rate Equation. *IEEE J Photovolt* 2013;3:1265-1270.
- [19] Schubert MC, Habenicht H, Warta W. Imaging of Metastable Defects in Silicon. *IEEE J Photovolt* 2011;1:168-173.
- [20] Søndenå R, Ghaderi A. Quantification of LID in multicrystalline silicon wafers. in 29<sup>th</sup> EUPVSEC 2014 Amsterdam, The Netherlands.
- [21] Shockley W, Read WT. Statistics of the recombinations of holes and electrons. *Phys Rev* 1952;87:835-842.
- [22] Hall RN. Electron-hole recombination in Germanium. *Phys Rev* 1952;87:387.
- [23] Hasebe M, Takeoka Y, Shinoyama S, Naito S. Formation process of stacking faults with ringlike distribution in CZ-Si wafers. *Jpn J Appl Phys* 1989;28:L1999-L2002.
- [24] Harada K, Furuya H, Kida M. Effects of thermal history on the formation of oxidation-induced stacking fault nuclei in Czochralski silicon during crystal growth. *Jpn J Appl Phys* 1997;36:3366-3373.

- [25] Trupke T, Bardos RA, Schubert MC, Warta W. Photoluminescence imaging of silicon wafers. *Appl Phys Lett* 2006;89:44107-3.
- [26] Walter D, Lim B, Bothe K, Falster R, Voronkov VV, Schmidt J. Impact of crystal growth on boron-oxygen defect formation. in 27th EUPVSEC 2012 Frankfurt, Germany.
- [27] Macdonald D, Deenapanray PNK, Cuevas A, Diez S, Glunz SW. The role of silicon interstitials in the formation of boron-oxygen defects in crystalline silicon. *Solid State Phenom* 2005;108-109:497-502.
- [28] Rein S, Diez S, Falster R, Glunz SW. Quantitative correlation of the metastable defect in Cz-silicon with different impurities. in 3rd WCPEC 2003 Osaka, Japan.
- [29] Rein S, Glunz SW. Electronic properties of the metastable defect in boron-doped Czochralski silicon: Unambiguous determination by advanced lifetime spectroscopy. *Appl Phys Lett* 2003;82:1054-1056.
- [30] Schmidt J, Cuevas A. Electronic properties of light-induced recombination centers in boron-doped Czochralski silicon. *J Appl Phys* 1999;86:3175-3180.
- [31] Hallam B, Abbott M, Nærland T, Wenham S. Fast and slow lifetime degradation in boron-doped Czochralski silicon described by a single defect. *Phys Status Solidi - Rapid Res Lett* 2016;10:520-524.